Quantifying Transient Ischemic Dilation Using Gated SPECT

Thomas F. Heston, MD; and Daniel M. Sigg, MD, PhD

Northwest Molecular, Kellogg, Idaho

Transient ischemic dilation (TID) is both a sensitive and a specific indicator of triple-vessel coronary artery disease. This finding, obtained from ungated SPECT images, is the ratio of the average ventricular size after stress compared with rest. With gated SPECT, however, measurements of the end-diastolic volume (EDV) and end-systolic volume (ESV) can be obtained, and the relative contributions of each to the TID ratio may be estimated. The objective of this study was to quantify the relative contributions of the EDV and ESV when correlating an optimized stress-induced volume ratio (SIVR) with myocardial ischemia. **Methods:** A retrospective review was made of 422 consecutive patients undergoing gated SPECT myocardial perfusion imaging. Semiquantitative summed stress and rest scores were determined using a 17-segment, 5-point model. The presence of myocardial ischemia was defined as a summed difference score of ≥ 3 (i.e., myocardial ischemia of $>4\%$). Poststress-to-rest ratios of the EDV, ESV, and left ventricular ejection fraction (LVEF) were correlated with myocardial ischemia. Using a brute force method, relative weights were assigned empirically to the EDV and ESV to calculate an optimized SIVR having the strongest correlation with myocardial ischemia. **Results:** There was a significant correlation between the presence or absence of ischemia and the ESV ratio ($P < 0.01$), the EDV ratio ($P < 0.01$), and the LVEF ratio ($P < 0.05$). When controlling for age, type of stress, and sex, the strongest correlation was with the ESV ratio. The SIVR most strongly correlated with myocardial ischemia was found to be the stress-to-rest ratio of the (ESV $\times$ 5.0 + EDV). This SIVR was more strongly correlated with myocardial ischemia than the stress-to-rest ESV ratio, EDV ratio, or LVEF ratio. **Conclusion:** Compared with either the ESV or the EDV stress-to-rest ratio alone, the combination of both results in a stronger correlation with myocardial ischemia. The contribution of the ESV was found to be 5 times greater than the contribution of the EDV when determining a SIVR most strongly correlated with stress-induced myocardial perfusion defects.

Key Words: transient ischemic dilation; myocardial ischemia; gated SPECT

Transient ischemic dilation (TID), loosely defined as the stress-induced apparent increase in the size of the left ventricle visualized by myocardial perfusion scintigraphy, has been shown in numerous studies to correlate with critical multivessel stenosis (*1–7*) and an increased risk of adverse outcomes (*8–10*), even in the absence of significant perfusion defects (*11,12*). TID has been observed in a variety of settings, after exercise as well as after pharmacologic stress, in planar projection imaging and SPECT, and in combination with all commercially available single-photon myocardial flow tracers. The mechanism for TID appears to be multifactorial, with subendocardial ischemia (*13–16*), temporary systolic dysfunction (*17*), and a true increase in the size of the left ventricle (*18*) having been proposed as explanations for the phenomenon. The diagnostic and prognostic utility of TID in myocardial perfusion scintigraphy has been recently reviewed (*19*).

As a result of averaging over the cardiac cycle, the assessment of TID in nongated studies receives roughly equal contributions from both the systolic and the diastolic intervals, with the diastolic component likely contributing more weight at slower resting heart rates, such as in patients who are taking β-blockers.

Here, we use the Quantitative Gated SPECT software package (QGS; Cedars-Sinai Medical Center, Los Angeles, CA) to determine the optimal weighting of endocardial end-systolic volume (ESV) and end-diastolic volume (EDV) that maximizes the correlation between a derived stress-induced volume ratio (SIVR) and the degree and extent of ischemia as quantified by the summed difference score (SDS). Although we cannot demonstrate it in this preliminary study, it is hoped that the optimized TID value allows better discrimination among high- and low-risk patients than the nongated measure of TID by providing a more accurate gauge of critical multivessel stenosis.

MATERIALS AND METHODS

Study Population

The study population consisted of 422 consecutive patients referred for rest–stress myocardial perfusion imaging in an outpatient setting between July 2003 and November 2004.

Imaging Protocol

Image acquisition was performed following imaging guidelines from the American Society of Nuclear Cardiology (20). A same-day, single-isotope (99mTc-tetrofosmin) protocol was used. Images were obtained using a single-head γ-camera (Orbiter 3700; Siemens Medical Systems, Inc.) using a 180° orbit from the −45° right anterior oblique view to the 135° left posterior oblique view. The camera was peaked at 140 keV using a 20% window. On the rest images, 32 stops at 40 s each were obtained, and after stress 64 stops at 20 s each were obtained. Patients received approximately 370 MBq of 99mTc-tetrofosmin 30 min before rest imaging. Both the rest and poststress images were gated. All datasets were acquired on the ICON workstation (Siemens Medical Systems, Inc.) and processed using the QGS software package (Cedars-Sinai Medical Center).

Exercise Stress Protocol

After rest imaging, patients able to exercise to at least 5 metabolic equivalents (METS) performed a treadmill exercise test. Patients unable to achieve a heart rate equal to 85% of their predicted maximum, unable to achieve a workload of 5 METS, or unable to exercise at least 3 min were converted to dipyridamole stress. The standard Bruce protocol was used whenever possible; however, the treadmill's speed and incline were often manually adjusted to match the patient's particular gait and walking ability (as long as the necessary workload and heart rate were achieved). Electrocardiographic monitoring was performed continuously. Twelve-lead electrocardiograms and blood pressure were obtained at each level of exercise. Exercise was continued to at least 85%, but not >100% of the patient's predicted maximum. Near maximal stress, approximately 1,300 MBq of 99mTc-tetrofosmin were injected. Patients then continued the exercise protocol for an additional 1–2 min, followed by a 1-min cool-down period during which the patient walked at 1.6 km/h on a level incline. Poststress images were started at approximately 20 min after tracer injection.

Dipyridamole Stress Protocol

Patients were instructed not to consume caffeine-containing products for at least 24 h and ideally 48 h before their scheduled appointment. Consumption of caffeinated products within 12 h before the test was an absolute contraindication. All patients underwent continuous electrocardiographic monitoring. Dipyridamole was injected over 4 min at a rate of 0.142 mg/kg/min. At 7 min (3 min after cessation of the dipyridamole infusion), approximately 1,300 MBq of 99mTc-tetrofosmin were injected, followed 2 min later by 75–150 mg of aminophylline as necessary to reduce patient side effects. Imaging was performed approximately 30 min after tracer injection. Whenever possible, dipyridamole testing was combined with light exercise (walking 2.4 km/h at a flat incline) to reduce side effects and decrease hepatic activity on subsequent imaging.

Image Interpretation

All scans were reviewed in the following manner: (a) the raw planar projection images were reviewed, (b) the QGS-derived ventricular volumes, wall motion, and wall thickening data were reviewed, and, finally, (c) the ungated short-axis, vertical long-axis, and horizontal long-axis slices were reviewed. Stress electrocardiograms were reviewed in conjunction with the nuclear scan images. A single experienced nuclear cardiologist with level 3 training in nuclear cardiology (21) performed all stress tests and interpreted all scans.

The summed stress score (SSS) and summed rest score (SRS) were determined semiquantitatively on all patients using a 17-segment, 5-point scale (22). The summed difference score (SDS) was calculated as the SSS − SRS. Patients with a SDS of ≥3 were defined as having myocardial ischemia. On a 17-segment, 5-point model, this equates to a reversible defect affecting >4% of the myocardium.

Statistical Analysis

Statistical analysis was performed using the SPSS Statistical Package 11.0 (SPSS, Inc.). Correlations were calculated between the presence or absence of myocardial ischemia, the SDS, the stress-to-rest ESV ratio, the stress-to-rest EDV ratio, and the stress-to-rest LVEF ratio. Pearson bivariate and partial correlation coefficients were used to determine the correlation between the variables examined. Averages are expressed as the mean ± 1 SD. An independent samples t test was used to compare means, with equal variances not assumed and 2-tailed P values calculated.

Determining Optimized Stress-Induced Volume Ratio

After correlations between myocardial ischemia and the EDV and ESV stress-to-rest ratios were calculated, a brute force method was used to determine if there was a ventricular volume ratio that was more strongly correlated with myocardial ischemia than either the EDV or ESV. This involved empirically giving a weight to the ESV value (Z) and then manually modifying this weight until a value for the SIVR was found that was maximally correlated with myocardial ischemia across the entire dataset for all patients.

We used the following formula as the definition of SIVR as a function of Z:

$$\text{SIVR}(Z) = \frac{\text{stress}(ESV \cdot Z + EDV)}{\text{rest}(ESV \cdot Z + EDV)}. \qquad \text{Eq. 1}$$

With Z set to 0, the SIVR equals the stress-to-rest EDV ratio, and when Z is infinitely large, the SIVR equals the stress-to-rest ESV ratio. With Z < 1, the SIVR is weighted toward EDV. With Z = 1, the ESV and EDV contribute equally to the SIVR, and with Z > 1, the SIVR is weighted toward the ESV.

Various values for Z were assigned, and the SIVR calculated. This SIVR(Z) was then correlated with myocardial ischemia. The values for Z were then plotted on the x-axis and the corresponding Pearson correlation coefficient of the SIVR(Z) was plotted on the y-axis to determine if a pattern would emerge (Fig. 1).

RESULTS

Patient Characteristics

The average patient age was 63 ± 13 y, 46% of whom were men and 54% were women. Stress was performed using dipyidamole in 37% and exercise testing in 63% of the patients.

The average defect size at stress affected 5.7% ± 8.4% of the myocardium (SSS = 3.9 ± 5.7). The average defect size at rest affected 5.1% ± 7.9% of the myocardium (SRS = 3.5 ± 5.4) and the average reversible defect affected 0.6% ± 4.3% of the myocardium (SDS = 0.41 ± 2.9). When cases of reverse redistribution defects were excluded (SDS < 0), the average reversible defect affected 4.7% ± 4.1% of the myocardium. Overall, 15% ± 36% of patients
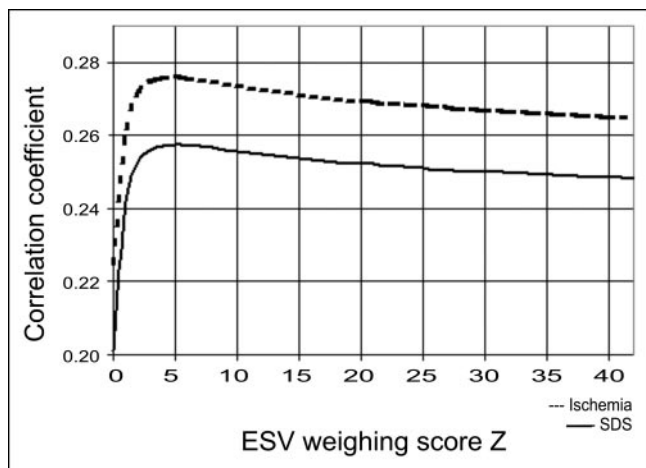
FIGURE 1. Relationship between ESV weighing factor Z, myocardial ischemia, and SDS as determined by their correlation coefficient after correcting for type of cardiac stress performed. When Z = 5, correlation is greater than either stress-to-rest EDV ratio (Z = 0) or stress-to-rest ESV ratio (Z = ∞).

FIGURE 2. After correcting for type of cardiac stress performed, correlation coefficient between myocardial ischemia and ESV weighing factor Z reaches its peak when Z value is between 4.6 and 5.

were classified as having myocardial ischemia—that is, they had a reversible defect affecting >4% of the myocardium. Patient characteristics grouped by the presence or absence of myocardial ischemia (SDS ≥ 3) are summarized in Table 1.

Optimized Stress-Induced Volume Ratio

Correlation coefficients for the relationship between the SIVR(Z) and myocardial ischemia, after controlling for type of stress (pharmacologic or exercise), are illustrated in Figure 1. This shows that correlation coefficients were higher when looking at the binary outcome of the presence or absence of myocardial ischemia than the ordinal variable SDS. However, both curves peak at a Z value of approximately 5.

Figure 2 zooms in on Z values at the peak of the curve in Figure 1. This graph shows that the highest correlation coefficient occurs when Z is set to a value between 4.6 and 5. The mean SIVR(5) in patients without ischemia was found to be 0.87 ± 0.16, resulting in an upper limit of normal equal to 1.19 (mean + 2 SDs). After determining that the SIVR(5) resulted in the highest coefficient for the
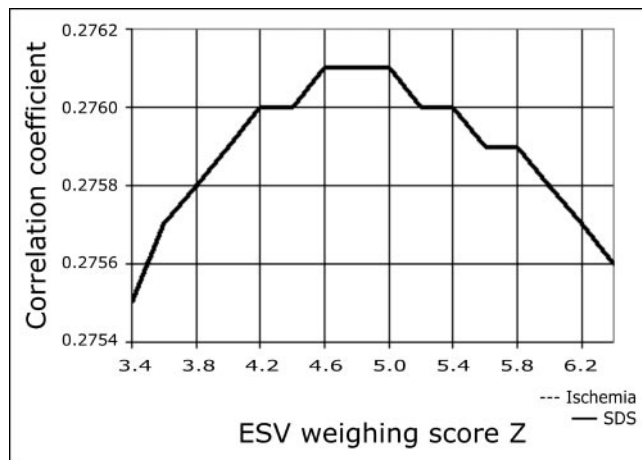
correlation with ischemia after controlling for type of stress, this value was then compared with the stress-to-rest EDV, ESV, and LVEF ratios.

The left ventricular volumes and ratios, grouped by sex, are summarized in Table 2. The average ventricular volumes are significantly smaller in women as compared with men, and the average LVEF is greater in women as compared with men. However, the ratios of ventricular volume and ejection fraction are not significantly different.

Table 3 summarizes the ventricular volumes and volume ratios in patients with and without myocardial ischemia, demonstrating that the SIVR(5) performs at least as well as the other ventricular volume ratios in separating ischemic from nonischemic patients. Note that the SIVR(5) in patients with ischemia was significantly higher in those undergoing dipyridamole stress compared with those undergoing treadmill stress (1.09 vs. 0.95; $P = 0.02$). Thus, the decision to optimize the SIVR(Z) after controlling for the type of stress performed was appropriate.

TABLE 1
Patient Characteristics Grouped by Presence or Absence of Myocardial Ischemia

Variable	No ischemia	Ischemia	P value
Age (y)	62.6 ± 13.4	66.5 ± 13.4	0.25
Male (%)	54	44	NS
Treadmill stress (%)	64	58	NS
SSS	2.9 ± 4.9	9.2 ± 6.6	0.001
SRS	3.4 ± 5.3	3.7 ± 5.9	NS

NS = not significant.

TABLE 2
Ventricular Volumes and Volume Ratios Grouped by Sex

Variable	Women	Men	P value
Stress ESV (mL)	19.4 ± 31.4	38.4 ± 35.0	0.001
Rest ESV (mL)	22.5 ± 31.7	42.8 ± 33.9	0.001
Stress EDV (mL)	54.1 ± 35.9	85.5 ± 43.7	0.001
Rest EDV (mL)	58.2 ± 36.5	92.2 ± 43.1	0.001
Stress LVEF (%)	71.0 ± 14.0	59.5 ± 11.4	0.001
Rest LVEF (%)	67.2 ± 13.1	57.2 ± 10.2	0.001
Stress/rest ESV ratio	0.84 ± 0.29	0.88 ± 0.18	NS
Stress/rest EDV ratio	0.93 ± 0.14	0.92 ± 0.11	NS
Stress/rest LVEF ratio	1.06 ± 0.13	1.04 ± 0.11	NS
SIVR(5)	0.87 ± 0.20	0.89 ± 0.15	NS

NS = not significant.

TABLE 3
TABLE 3
Ventricular Volumes and Volume Ratios Grouped by
Presence or Absence of Myocardial Ischemia

Variable	No ischemia	Ischemia	P value
Stress ESV (mL)	26.5 ± 33.6	35.4 ± 24.6	0.01
Rest ESV (mL)	30.5 ± 33.5	35.6 ± 24.3	NS
Stress EDV (mL)	66.3 ± 41.7	80.7 ± 35.9	0.05
Rest EDV (mL)	71.8 ± 42.1	80.7 ± 34.7	NS
Stress LVEF (%)	66.7 ± 13.9	59.8 ± 12.0	0.001
Rest LVEF (%)	63.4 ± 12.9	59.4 ± 12.3	0.02
Stress/rest ESV ratio	0.84 ± 0.23	1.02 ± 0.29	0.001
Stress/rest EDV ratio	0.92 ± 0.12	1.00 ± 0.14	0.001
Stress/rest LVEF ratio	1.06 ± 0.12	1.02 ± 0.13	0.03
SIVR(5)	0.87 ± 0.16	1.01 ± 0.22	0.001

NS = not significant.

The stress-induced ventricular volume ratios were also normalized for ischemic patients relative to nonischemic patients. The normalized ratios of ESV (ESVr), EDV (EDVr), and LVEF (LVEFr) are as follows: ESVr = 1.02/0.84 = 1.21; EDVr = 1.00/0.92 = 1.07; and LVEFr = 1.02/1.06 = 0.96. Thus, ischemia resulted in a mean increase in ESVr of 21% relative to nonischemic patients, whereas changes in EDVr and LVEFr were only 7% and −4%, respectively.

DISCUSSION

Previous studies have demonstrated the diagnostic and prognostic utility of nongated or time-averaged TID in patients with coronary artery disease. In a recent prospective study looking at 177 patients undergoing dual-isotope, adenosine stress gated SPECT, the sensitivity and specificity of detecting critical multivessel or left anterior descending artery stenosis using nongated TID were 71% and 86%, respectively (7). In this study we performed rest and stress gated SPECT myocardial perfusion images in 422 consecutive patients and found that incorporating information from gated imaging has significant impact on the correlation between TID and measures of ischemia.

There is little research looking at the use of both stress and rest gated images in evaluating changes in left ventricular volume. Bestetti et al. (17), who likewise used gated ^{99m}Tc-tetrofosmin SPECT, demonstrated that in patients with significant perfusion defects and an apparent 5% or greater drop in poststress LVEF ("stunned" group), there was a 26% increase in mean ESV stress-to-rest ratio (ESVr) compared with patients with perfusion defects and a <5% increase in LVEF. The increase in the mean EDV stress-to-rest ratio (EDVr) was less pronounced (6%). The patients demonstrating stunning also had a significantly greater ischemia quantified by SDS compared with nonstunned patients, raising the possibility that gated SIVR measurements correlate with level of ischemia. Here, we demonstrate that a significant correlation exists between all pairings of SDS

with ESVr, EDVr, and LVEFr, but ESVr is most highly correlated with ischemia, whereas LVEFr is least correlated. The stress-to-rest ratio of a linear combination of ESV and EDV weighted 5-fold toward ESV (Z = 5) exhibits the highest correlation with SDS measurements. Although nongated TID measurements were not included in this study, one might expect that time-averaged stress-to-rest endocardial volume ratios demonstrated less correlation with ischemia because, in most resting patients (note that patients are at rest even during poststress imaging), the cardiac cycle spends a greater proportion of time in diastole, and, therefore, nongated TID measurements are weighted on average more toward EDV than ESV.

It has been well documented that cutoff values for an abnormal TID vary widely throughout the literature, ranging from 1.012 to 1.36 (1–2,5–7). Part of the variability arises from the use of different isotopes for rest and stress studies (5,7), time to imaging after stress (relevant to thallium studies), different types of stress, and other factors. In our hands, patients without ischemia demonstrated a significant decrease in ESV and EDV after stress (EDVr, ESVr < 1), and an increase in the LVEF. The decrease in ESV was the largest proportional change (ESVr = 0.84 compared with EDVr = 0.92, and LVEFr = 1.06). The reason for this deviation from unity in nonischemic patients is presumably due to the physiologic demand for an increased cardiac output after stress, which depends on both the heart rate and stroke volume. It is important to note the important role of the ESV in patients both with and without ischemia. In nonischemic patients, the change in the ESV appeared to play a primary role in meeting the increased physiologic demand. In patients with ischemia, the ESV changes were the most strongly correlated with perfusion defects. Furthermore, the change in the ESVr (+21%) in ischemic compared with nonischemic patients was much greater than the changes observed in the EDVr (+7%) and the LVEFr (−4%). These findings all lead to the conclusion that the ESV plays a central role in describing the physiologic changes to cardiac stress in both ischemic and nonischemic patients. We found that the ESV appeared to be 5 times more important than the EDV but that both values are important.

A visual analysis of representative midventricular tomograms can further help demonstrate the increased importance of the ESV in the determination of the TID ratio. In Figure 3, a representative midventricular short-axis tomogram is shown at end-diastole and end-systole. The summed planar tomogram, which is not obtained from gated data and from which the TID ratio is derived, is shown on the right side of Figure 3. From this example, the relative impact of the ESV tomogram on the summed image appears to be much greater than the impact of the ESV tomogram. A semiquantitative analysis might even agree with our conclusion that the impact of the ESV is 5 times greater than the impact of the EDV on the summed image, from which the TID is derived.

FIGURE 3. Representative midventricular tomograms from end-diastole (left), end-systole (middle), and summed planar tomogram (right). There is an increased count density at end-systole compared with end-diastole, creating a much greater contribution to summed planar tomogram from which the TID ratio is derived.
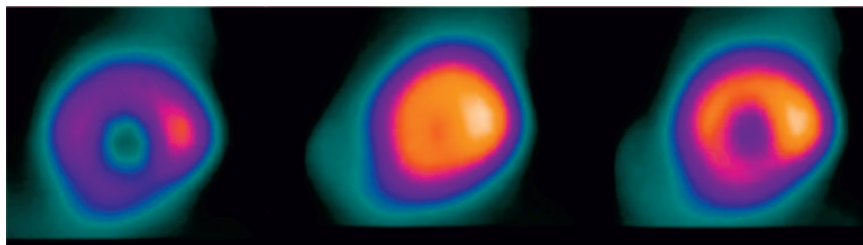
The mathematic basis for our results is suggested by the following formula obtained from differentiating the expression for LVEF = (EDV − ESV)/EDV:

$$-\frac{\Delta LVEF}{LVEF} \approx \left(\frac{\Delta ESV}{ESV} - \frac{\Delta EDV}{EDV}\right)\left(\frac{EDV}{ESV} - 1\right)^{-1}, \quad \text{Eq. 2}$$

where for any quantity X (representing the value at rest), $\Delta X = X_{stress} - X_{rest}$. For small changes in X, and recognizing $\Delta X/X \approx X_r - 1$, Equation 2 can be summarized as $1 - LVEF_r \approx (ESV_r - EDV_r)/(EDV/ESV - 1)$. Equation 2 predicts that for a small decrease in LVEF, $ESV_r > EDV_r$, which is what we have observed. On the other hand, if LVEF does not change in poststress imaging, then $ESV_r \approx EDV_r$. Because EDV is usually significantly greater than ESV, we also have in the usual cases, $(ESV_r - 1) > (1 - LVEF_r)$. Combining these statements with our results, one may conclude that, on average, TID is accompanied by a relative decrease in apparent LVEF, although it may be small. The variable that demonstrates the largest proportional increase is ESV_r, which is consistent with a Z factor of 5 in SIVR. Thus, a greater relative change in ESV is consistent with a reduction in the apparent ejection fraction, suggesting that transient systolic dysfunction or stunning may be an important component in TID. However, apparent wall thinning due to transient endocardial ischemia undoubtedly also plays a role, particularly in pharmacologically stressed patients (3,13).

It should be remarked that, although statistically significant because of the relatively large number of study participants (n = 422), the Pearson correlation coefficients comparing SIVR(Z) versus SDS are not large, even for the optimal value of Z = 5.

The weak correlation between SIVR(5) and SDS can be expected if one considers the many sources of variability, both biologic and technical, that are possible. Biologic sources of variability may include the development of collateral vessels in adapting to ischemia, the degree of left ventricular hypertrophy (23,24), and heart size. The latter is a well-known source of error that arises from the limited resolution of the detection system (25,26). It is evident from our data that a significant difference exists between men and women in the apparent size of the left ventricular chamber sizes and the calculated LVEF (Table 2). However, there was not a significant difference between the sexes when stress-to-rest ratios of volumes or LVEF were computed,

perhaps because confounding factors canceled one another out.

Other sources of possible technical error are myriad. These include patient motion, extracardiac hot spots (27), cardiac arrhythmia (28), attenuation artifact, and reconstruction or processing errors. Advances in scanning technology, such as the merging of anatomic imaging with SPECT, will minimize some sources of error, such as attenuation artifact, and provide a reliable method of determining true volume size.

As it stands now, the use of automated quantification of ventricular volume from nongated static (i.e., time-averaged over the cardiac cycle) SPECT perfusion images has been validated against measurements of left ventricular cavity volume by echocardiography (29), first-pass radionuclide angiography (30), and MRI (31). This is important because, although software that automatically quantifies TID can be cost prohibitive, the majority of commercial myocardial perfusion quantification programs have automated border-finding algorithms that will estimate endocardial ESV and EDV. The validity of absolute quantification of left ventricular cavity volume using SPECT perfusion imaging has been questioned (7) because of lack of evidence. Despite this, volume estimation has been shown to be reproducible using a variety of protocols (27,32). Thus, stress-to-rest volume ratios such as used here to compute SIVR(Z) are likely to be accurate independently of the sources of error listed. This has been demonstrated in the computation of LVEF using different software algorithms (33).

Our study has several limitations. It has been hypothesized in the literature in an editorial (34) and in a phantom study (35) that changes in ventricular volumes are influenced by changes in endocardial edge detection when significant perfusion defects are present. However, there are human studies that challenge this hypothesis (36,37). Others have only shown discrepancies with radionuclide angiography when ventricular volumes are >200 mL (38). Furthermore, our average perfusion defect size was much smaller than the ones created in the phantom study, and, thus, its results are unlikely to apply to our patient population. However, we allow that edge detection artifacts add to the variability in our volume estimates.

Another limitation was the inability of our clinic to correlate the ventricular volume ratios with the QGS-derived TID ratios. Because this proprietary software upgrade to our

system was not available at the time of this study, a direct correlation between the SIVR(5) and TID is not possible using our data. However, we nevertheless believe that the concept of using stress-induced volume ratios derived from the gated SPECT data may ultimately provide a greater understanding of the ventricular changes in response to stress.

Finally, we made the decision to correlate the SIVR with perfusion defect scores instead of angiography or CT calcium scoring. Because myocardial ischemia is thought to be the foundation of an elevated TID ratio, correlating the SIVR with these anatomic (as opposed to physiologic) imaging studies could lead to misleading results. Other researchers have recently published their findings relating to the correlation between TID, SIVR, and perfusion defects (*39,40*). They have concluded that the ESV is the primary factor affecting the TID ratio and change in LVEF among patients with myocardial ischemia. Our findings are relevant because we provide a starting point for quantifying the relative contributions of the ESV and the EDV to stress-induced changes in the TID ratio and LVEF in patients with myocardial ischemia.

CONCLUSION

The computation of a stress-induced volume ratio, derived from a combination of the EDV and ESV, is more strongly correlated with myocardial ischemia than either the EDV or ESV ratio alone. In our patient population, the ESV appears to be approximately 5 times more important than the EDV when calculating an optimized stress-induced volume ratio. Future studies will be needed to validate gated measurements of the SIVR against nongated, time-averaged measures of TID and to determine whether gating leads to improved accuracy of detecting critical and extensive coronary artery disease.

ACKNOWLEDGMENT

REFERENCES

1. Weiss AT, Berman DS, Lew AS, et al. Transient ischemic dilation of the left ventricle on stress thallium-201 scintigraphy: a marker of severe and extensive coronary artery disease. *J Am Coll Cardiol.* 1987;9:752–759.

2. Chouraqui P, Rodrigues EA, Berman DS, Maddahi J. Significance of dipyridamole-induced transient dilation of the left ventricle during thallium-201 scintigraphy in suspected coronary artery disease. *Am J Cardiol.* 1990;66:689–694.

3. Takeishi Y, Tono-oka I, Ikeda K, Komatani A, Tsuiki K, Yasui S. Dilatation of the left ventricular cavity on dipyridamole thallium-201 imaging: a new marker of triple-vessel disease. *Am Heart J.* 1991;121:466–475.

4. Toyama T, Caner BE, Tamaki N, et al. Transient ischemic dilatation of the left ventricle observed on dipyridamole-stressed thallium-201 scintigraphy [in Japanese]. *Kaku Igaku.* 1993;30:605–611.

5. Mazzanti M, Germano G, Kiat H, et al. Identification of severe and extensive coronary artery disease by automatic measurement of transient ischemic dilation of the left ventricle in dual-isotope myocardial perfusion SPECT. *J Am Coll Cardiol.* 1996;27:1612–1620.

6. Kinoshita N, Sugihara H, Adachi Y, et al. Assessment of transient left ventricular dilatation on rest and exercise on Tc-99m tetrofosmin myocardial SPECT. *Clin Nucl Med.* 2002;27:34–39.

7. Abidov A, Bax JJ, Hayes SW, et al. Integration of automatically measured transient ischemic dilation ratio into interpretation of adenosine stress myocardial perfusion SPECT for detection of severe and extensive CAD. *J Nucl Med.* 2004;45:1999–2007.

8. McClellan JR, Travin MI, Herman SD, et al. Prognostic importance of scintigraphic left ventricular cavity dilation during intravenous dipyridamole technetium-99m sestamibi myocardial tomographic imaging in predicting coronary events. *Am J Cardiol.* 1997;79:600–605.

9. Lette J, Bertrand C, Gossard D, et al. Long-term risk stratification with dipyridamole imaging. *Am Heart J.* 1995;129:880–886.

10. Krawczynska EG, Weintraub WS, Garcia EV, Folks RD, Jones ME, Alazraki NP. Left ventricular dilatation and multivessel coronary artery disease on thallium-201 SPECT are important prognostic indicators in patients with large defects in the left anterior descending distribution. *Am J Cardiol.* 1994;74:1233–1239.

11. Abidov A, Bax JJ, Hayes SW, et al. Transient ischemic dilation ratio of the left ventricle is a significant predictor of future cardiac events in patients with otherwise normal myocardial perfusion SPECT. *J Am Coll Cardiol.* 2003;42:1818–1825.

12. Choong KK, Russell PA. Transient left ventricular dilatation in the absence of epicardial disease on angiography. *Clin Nucl Med.* 2004;29:348–351.

13. Iskandrian AS, Heo J, Nguyen T, Lyons E, Paugh E. Left ventricular dilatation and pulmonary thallium uptake after single-photon emission computer tomography using thallium-201 during adenosine-induced coronary hyperemia. *Am J Cardiol.* 1990;66:807–811.

14. Sugihara H, Shiga K, Umamoto I, et al. Assessment of transient dilation of the left ventricular cavity in patients with hypertrophic cardiomyopathy by exercise thallium-201 scintigraphy [in Japanese]. *Kaku Igaku.* 1990;27:1281–1289.

15. Hansen CL, Sangrigoli R, Nkadi E, Kramer M. Comparison of pulmonary uptake with transient cavity dilation after exercise thallium-201 perfusion imaging. *J Am Coll Cardiol.* 1999;33:1323–1327.

16. Marcassa C, Galli M, Baroffio C, Campini R, Giannuzzi P. Transient left ventricular dilation at quantitative stress-rest sestamibi tomography: clinical, electrocardiographic, and angiographic correlates. *J Nucl Cardiol.* 1999;6:397–405.

17. Bestetti A, Di Leo C, Alessi A, Triulzi A, Tagliabue L, Tarolo GL. Post-stress end-systolic left ventricular dilation: a marker of endocardial post-ischemic stunning. *Nucl Med Commun.* 2001;22:685–693.

18. Kurata C, Wakabayashi Y, Shouda S, Mikami T, Tawarahara K. Quantification of left ventricular size on exercise thallium-201 single-photon emission tomography. *Eur J Nucl Med.* 1996;23:762–767.

19. McLaughlin MG, Danias PG. Transient ischemic dilation: a powerful diagnostic and prognostic finding of stress myocardial perfusion imaging. *J Nucl Cardiol.* 2002;9:663–667.

20. American Society of Nuclear Cardiology. Updated imaging guidelines for nuclear cardiology procedures: part 1. *J Nucl Cardiol.* 2001;8:G5–G58.

21. Beller GA, Bonow RO, Fuster V. Core Cardiology Training Symposium (COCATS): ACC revised recommendations for training in adult cardiovascular medicine—Core Cardiology Training II (COCATS 2) (revision of the 1995 COCATS training statement). *Am Coll Cardiol.* 2002;39:1242–1246.

22. Cerqueira MD, Weissman NJ, Dilsizian V, et al. Standardized myocardial segmentation and nomenclature for tomographic imaging of the heart: a statement for healthcare professionals from the Cardiac Imaging Committee of the Council on Clinical Cardiology of the American Heart Association. *Circulation.* 2002;105:539–542.

23. Hardebeck CJ. Transient ischemic dilation. *J Am Coll Cardiol.* 2004;44:211–212.

24. Hittinger L, Mirsky I, Shen YT, Patrick TA, Bishop SP, Vatner SF. Hemodynamic mechanisms responsible for reduced subendocardial coronary reserve in dogs with severe left ventricular hypertrophy. *Circulation.* 1995;92:978–986.

25. Nichols K, DePuey EG, Friedman MI, Rozanski A. Do patient data ever exceed the partial volume limit in gated SPECT studies? *J Nucl Cardiol.* 1998;5:484–490.

26. Feng B, Sitek A, Gullberg GT. Calculation of the left ventricular ejection fraction without edge detection: application to small hearts. *J Nucl Med.* 2002;43:786–794.

27. Vallejo E, Dione DP, Bruni WL, et al. Reproducibility and accuracy of gated SPECT for determination of left ventricular volumes and ejection fraction: experimental validation using MRI. *J Nucl Med.* 2000;41:874–882.

28. Nichols K, Dorbala S, DePuey EG, Yao SS, Sharma A, Rozanski A. Influence of arrhythmias on gated SPECT myocardial perfusion and function quantification. *J Nucl Med.* 1999;40:924–934.

29. Nichols K, Lefkowitz D, Faber T, et al. Echocardiographic validation of gated SPECT ventricular function measurements. *J Nucl Med.* 2000;41:1308–1314.

30. Williams KA, Taillon LA. Left ventricular function in patients with coronary artery disease assessed by gated tomographic myocardial perfusion images: comparison with assessment by contrast ventriculography and first-pass radionuclide angiography. *J Am Coll Cardiol.* 1996;27:173–181.

31. Faber TL, Cooke CD, Folks RD, et al. Left ventricular function and perfusion from gated SPECT perfusion images: an integrated method. *J Nucl Med*. 1999; 40:650–659.

32. Nakata T, Katagiri Y, Doawara Y, et al. Two- and three-dimensional assessments of myocardial perfusion and function by using technetium-99m sestamibi gated SPECT with a combination of count- and image-based techniques. *J Nucl Cardiol*. 2000;7:623–632.

33. Hambye AS, Vervaet A, Dobbeleir A. Variability of left ventricular ejection fraction and volumes with quantitative gated SPECT: influence of algorithm, pixel size and reconstruction parameters in small and normal-sized hearts. *Eur J Nucl Med Mol Imaging*. 2004;31:1606–1613.

34. Bonow RO. Gated myocardial perfusion imaging for measuring left ventricular function. *J Am Coll Cardiol*. 1997;30:1649–1650.

35. Manrique A, Hitzel A, Brasse D, Vera P. Effect of perfusion pattern and imaging sequence on gated perfusion SPECT evaluation of myocardial stunning. *J Nucl Med*. 2005;46:176–183.

36. Everaert H, Bossuyt A, Franken PR. Left ventricular ejection fraction and volumes from gated single photon emission tomographic myocardial perfusion images: comparison between two algorithms working in three-dimensional space. *J Nucl Cardiol*. 1997;4:472–476.

37. Chua T, Yin LC, Thiang TH, Choo TB, Ping DZ, Leng LY. Accuracy of the automated assessment of left ventricular function with gated perfusion SPECT in the presence of perfusion defects and left ventricular dysfunction: correlation with equilibrium radionuclide ventriculography and echocardiography. *J Nucl Cardiol*. 2000;7:301–311.

38. Vanhove C, Walgraeve N, De Geeter F, Franken PR. Gated myocardial perfusion tomography versus gated blood pool tomography for the calculation of left ventricular volumes and ejection fraction. *Eur J Nucl Med Mol Imaging*. 2002; 29:735–741.

39. Hung GU, Lee KW, Chen CP, Lin WY, Yang KT. Relationship of transient ischemic dilation in dipyridamole myocardial perfusion imaging and stress-induced changes of functional parameters evaluated by Tl-201 gated SPECT. *J Nucl Cardiol*. 2005;12:268–275.

40. Del Val Gomez M, Gallardo FG, San Martin MA, Garcia A, Terol I. Ischaemic related transitory left ventricular dysfunction in ^{201}Tl gated SPECT. *Nucl Med Commun*. 2005;26:601–605.